Exosomal microRNA-4516, microRNA-203 and SFRP1 are potential biomarkers of acute myocardial infarction

PENG LIU[1*], SHUYA WANG[1*], KAIYUAN LI[2*], YANG YANG[3], YILONG MAN[1], FENGLI DU[1,4], LEI WANG[1], JING TIAN[1] and GUOHAI SU[1]

[1]Department of Cardiovascular Medicine, Central Hospital Affiliated to Shandong First Medical University, Jinan Central Hospital, Jinan, Shandong 250000; [2]Dalian Medical University, Dalian, Liaoning 116000; [3]Department of Cardiovascular Medicine, Affiliated Hospital of Jining Medical University, Jining, Shandong 272000; [4]Department of Cardiovascular Medicine, Shandong Provincial Public Health Centre, Jinan, Shandong 250000, P.R. China

Received November 21, 2022; Accepted April 20, 2023

DOI: 10.3892/mmr.2023.13010

Abstract. Acute myocardial infarction (AMI) is a serious disease which threatens public health. Exosomes (exos) contain certain genetic information and are important communication vehicles between cells. In the present study, different exosomal microRNAs (miRs), which exhibit a notable association between expression levels in plasma and AMI were assessed to support the development of new diagnostic and clinical assessment markers of patients with AMI. In total, 93 individuals, including 31 healthy controls and 62 patients with AMI, were recruited for the present study. Data on age, blood pressure, glucose levels, lipid levels and coronary angiography images were collected from the enrolled individuals, and plasma samples were collected. Plasma exos were extracted and verified using ultracentrifugation, transmission electron microscopy (TEM), nanoparticle tracking analysis (NTA) and western blotting (WB). Exo-miR-4516 and exo-miR-203 in plasma exos were identified by exosomal miRNA sequencing analysis, reverse transcription-quantitative PCR was performed to detect the levels of exo-miR-4516 and exo-miR-203 in plasma exos, and ELISA was performed to detect the levels of secretory frizzled-related protein 1 (SFRP1) in samples. The correlation analysis between exo-miR-4516, exo-miR-203 and SFRP1 in plasma exos and AMI was presented as receiver operating characteristic curves (ROCs) of the SYNTAX score, cardiac troponin I (cTnI), low-density lipoprotein (LDL) and each indicator separately. Kyoto Encyclopedia of Genes and Genomes enrichment analysis was performed to predict relevant enrichment pathways. Exos were successfully isolated from plasma by ultracentrifugation, which was confirmed by TEM, NTA and WB. Exo-miR-4516, exo-miR-203 and SFRP1 levels in plasma were significantly higher in the AMI group compared with the healthy control group. ROCs demonstrated that exo-miR-4516, exo-miR-203 and SFRP1 levels had a high diagnostic efficiency in predicting AMI. Exo-miR-4516 was positively correlated with SYNTAX score, and plasma SFRP1 was positively correlated with plasma cTnI and LDL. In conclusion, the data demonstrated that exo-miR-4516, exo-miR-203 and SFRP1 levels could be used in combination to diagnose and assess the severity of AMI. The present study was retrospectively registered (TRN, NCT02123004).

Correspondence to: Dr Guohai Su, Department of Cardiovascular Medicine, Central Hospital Affiliated to Shandong First Medical University, Jinan Central Hospital, 105 Jiefang Road, Jinan, Shandong 250000, P.R. China
E-mail: gttstg@163.com

*Contributed equally

Key words: exosome, microRNA-4516, microRNA-203, secretory frizzled-related protein 1, acute myocardial infarction

Introduction

Cardiovascular diseases (CVDs) are a series of heart and vascular diseases, which cause a huge social and economic burden worldwide. Acute myocardial infarction (AMI) is one important type of CVD (1). Mortality caused by CVD has been reported to account for 43.81 and 46.66% of total mortality in urban and rural areas respectively, and the mortality rate of AMI in China has risen (2). AMI is one common type of coronary heart disease, which is induced by acute and persistent ischemic hypoxia and ultimately causes myocardial necrosis (3). Traditionally, AMI has been diagnosed based on specific electrocardiogram (ECG) presentations and elevated cardiac serum markers, including lactate dehydrogenase, cardiac Troponin I (cTnI), cardiac muscle troponin T (cTnT) and creatine kinase MB (CK-MB) (4,5). However, the complexity of the condition of the patient, the onset of acute pericarditis, myocarditis, heart failure, hypertension and acute pulmonary embolism can also lead to elevated levels of existing markers, which makes distinguishing AMI from these conditions difficult (6,7). Only ST-segment elevation MI (STEMI) can be detected by electrocardiography, while the infarcted vessels cannot be predicted the first time. Although coronary angiography is the most effective method to diagnose and treat AMI, it may also be ineffective in certain cases where the infarcted vessels are complex. Furthermore, some areas do not have sufficient access to coronary angiography. This makes

it difficult for a large proportion of patients with AMI to receive the optimal treatment (8). In summary, it is necessary to develop more comprehensive clinical indicators to aid the diagnosis and assessment of AMI as quickly as possible.

Exosomes (exos) are endogenously formed extracellular vesicles that were first identified in the late 1960s (9) and are considered micro-vesicles with a diameter of 30-150 nm. Exos can be produced by numerous types of cells and are widely present in the urine, blood and saliva. Exos have a phospholipid bilayer structure and the micro-vesicles are rich in biomolecules, such as proteins, lipids, mRNA and non-coding RNA; therefore, exos can act as messengers, which mediate intercellular communication and participate in the regulation of cellular functions (10). Moreover, certain proteins have been previously detected in exos, which demonstrate superiority in the timeliness and specificity of different diseases compared with traditional plasma markers, and these exos display great clinical value by serving as novel biomarkers and therapeutic agents for certain neoplastic diseases. For example, it has been shown that ABCG1 and PTEN can be proteins in exosomes that delay the progression of atherosclerosis (11,12). In the study of cardiovascular system diseases, increasing attention has been paid to the implications and functions of exosomal microRNAs (miRNAs) (13).

miRNAs are a class of highly conserved small non-coding RNAs, which widely exist in plasma or serum, either bound to protein complexes or present in microvesicles or lipoproteins (14-16). miRNAs mainly regulate genes by binding to the 3'-UTR of mRNAs and interfering with subsequent protein synthesis. Numerous miRNAs have been reported to have an association with the pathogenesis of CVD (17,18). It has been previously demonstrated that miRNA-133 (miR-133) widely exists in cardiomyocytes, that the inhibition of miR-133 increases cardiac hypertrophy and upregulation of miR-133 improves cardiac function (19). miR-199a and miR-590 have been reported to alleviate cardiac function after AMI by inducing mitosis (20). Furthermore, in terms of the therapeutic study of miRNAs, inhibition of miR-92a reduces endothelial inflammation and promotes angiogenesis and the functional recovery of ischemic myocardium (21). It has been reported that exosomal miRNA levels and corresponding disease scores, such as the SYNTAX score, can be used to predict the complexity of coronary lesions, which provides valuable references for the next step of treatment (22,23).

The Wnt/β-catenin signaling pathway has been reported to be reactivated after MI and is involved in the regulation of pathophysiological processes, such as myocardial apoptosis and myocardial fibrosis (24-26). Secretory frizzled-related protein 1 (SFRP1) is a protein structurally similar to the frizzled (FZ) receptor that inhibits the binding of Wnt or FZ receptor/β-catenin signaling pathway activity. It has been previously suggested that SFRP1 is closely associated with myocardial fibrosis and cardiac remodeling, and it is unclear whether its expression is affected by MI (27-33).

In conclusion, studies on AMI and exosomal miRNA are rare; however, it is necessary to explore their association to facilitate the clinical diagnosis and assessment of AMI. The aim of the present study was to identify top differential miRNAs from sequencing results, and to validate these miRNAs in AMI and healthy control groups. The aim was also to identify new markers of AMI by performing correlation analysis between exosomal miRNAs and existing clinical indicators in AMI. Our previous study reported the involvement of miRNAs carried by exosomes in the formation of frontal atherosclerosis (34). This study will investigate the value of miR-4516 and miR-203 in aiding the diagnosis of acute myocardial infarction and predicting the extent of vascular injury through sequencing analysis. These will help in the future diagnosis and treatment in the clinic.

Materials and methods

Ethics approval. The present study was performed at The Central Hospital Affiliated with Shandong First Medical University (Jinan, China). Blood samples from patients with AMI and healthy controls were collected from The Department of Cardiovascular Medicine and The Emergency and Health Examination Center between October 2020 and May 2021. The present study was performed according to the principles of the Declaration of Helsinki, and the study design was approved by The Ethical Committee of The Central Hospital Affiliated with Shandong First Medical University (approval no. 2018-039-01; Jinan, China).

Study participants. All participants in the present study were volunteers and signed an informed consent form. Basic information about the participants, including sex, age, disease situation and other relevant personnel information were recorded. A total of 62 patients with AMI and 31 healthy controls were enrolled in the present study. The diagnostic criteria for acute myocardial infarction were defined by The Joint European Society of Cardiology (35). The main AMI diagnostic basis includes typical AMI symptoms and signs, abnormal ECG, the level of serum biomarkers and coronary angiography results (36).

Inclusion criteria. The inclusion criteria for selecting participants were as follows: i) Aged 35-75 years old; ii) no history of smoking or had quit smoking >3 months before the study; iii) chest pain lasting >30 min with no relief. The time window was within 12 h from the start of chest pain, including both acute ST elevation and non-ST elevation MI, with samples collected from the AMI group within 12 h of onset; iv) cTnT or cTnI >upper limit of a normal level (99th percentile of the upper reference value) for at least one-time point; v) patients with ≥70% stenosis of the pathogenic vessel identified by coronary angiography, as this was required for percutaneous coronary intervention (PCI); vi) no anticoagulants administered; and vii) systolic blood pressure level was 90-140 mmHg, and diastolic blood pressure was <90 mmHg (patients with a history of well-controlled hypertension were also enrolled). All patients with acute myocardial infarction were given standard treatment. The appropriate medical records were retrieved for all participants.

Exclusion criteria. The exclusion criteria for selecting participants for the present study were as follows: i) Presence of infection, autoimmune disease, liver or kidney dysfunction, or history of tumor; ii) aged <35 or >75 years old; iii) a blood glucose level of >7 mmol/l; iv) systolic blood pressure <90 or >140 mmHg and/or diastolic blood pressure >90 mmHg; and v) psychiatric disorders (37).

SYNTAX score. SYNATX scores were assigned by assigning scores to individual coronary vessels. The greater the sum of the scores, the more severe the lesion. The complexity of coronary lesions was quantitatively evaluated according to the integration system by two or more experienced physicians according to anatomical characteristics, such as lesion location, severity, bifurcation and calcification of the left main coronary artery and/or three main vessels (38).

Extraction of exos from blood samples. A fasting blood sample (5 ml in a Becton,Dickinson and Company EDTA anticoagulant tube) was collected from all members of the healthy control group, and 5 ml of venous blood was collected before emergency PCI from participants in the AMI group. After centrifugation at 2,000 x g at 4˚C for 10 min, plasma was collected in 1.5 ml RNase-free tubes and stored at -80˚C. After 16,260 x g centrifugation at 4˚C for 45 min, the supernatant of the plasma was collected and filtered using a 0.22 μm filter. The filtered supernatant was transferred into an ultracentrifuge tube and was centrifuged at 110,000 x g at 4˚C for 120 min. At the end of the first ultracentrifugation step, the supernatant was aspirated, and the pellet was resuspended in 100 μl sterile PBS. The aforementioned centrifugation parameters were repeated for further centrifugation steps. After the second ultracentrifugation, the supernatant was removed, and the pellet was resuspended in 100 μl PBS, transferred to a new RNase-free tube and stored in a -80˚C freezer.

Transmission electron microscopy (TEM) and nanoparticle tracking analysis (NTA) examination. A total of 10 μl exo suspension solution was dropped onto copper grids and subsequently transferred to 3% glutaraldehyde solution for fixation for 30 min, followed by the addition of 4% acetic acid oxygen dye solution and 1% methylcellulose solution, for visualization under TEM (ht-7700; Hitachi, Ltd.). Dilute exos obtained by ultracentrifugation were processed by NTA, to define the particle size distribution and exo concentration of all samples. Diluted exos obtained by ultracentrifugation were processed by NTA, to define the particle size distribution and exo concentration of all samples. The whole experiment was performed at 20-25˚C.

Western blotting (WB). RIPA lysis buffer (cat. no P0013B; Beyotime Institute of Biotechnology) was used to extract proteins from the exos previously isolated by ultracentrifugation. After ultrasonic cell disruptor processing, the lysate was centrifuged at 16,260 x g at 4˚C for 5 min, and the supernatant was collected for concentration quantification using a BCA assay kit. Loading buffer was added to the samples, the samples were boiled for 10 min, and then stored at -80˚C. A total of 20 μg protein sample per well was loaded on 10% sodium dodecyl sulfate-polyacrylamide gels. After electrophoresis was completed, the separated proteins were subsequently transferred onto a 0.22 μm PVDF membrane for 90 min at 70 V. The membranes were blocked with 5% non-fat milk powder (diluted in TBST with 0.1% Tween 20) at room temperature. After blocking, membranes were incubated with primary antibodies against CD9 (1:1,000; cat. no. 20597-1-AP; Proteintech Group, Inc.), Alix (1:1,000; cat. no. sc-53540; Santa Cruz Biotechnology, Inc.) and calnexin (1:1,000; cat. no. 10427-2-AP; Proteintech Group, Inc.) as a negative control, overnight at 4˚C. The membranes were washed three times using TBST and subsequently incubated with Anti-rabbit IgG (1:20,000; cat. no. 7074; Cell Signaling Technology, Inc.) and Anti-mouse IgG (1:20,000; cat. no. 7076; Cell Signaling Technology, Inc.) secondary antibodies for 60 min at room temperature. The chemiluminescence reagent was Immobilon Western (MilliporeSigma) and Images were captured using a Tanon 5200 Multi Chemiluminescent Imaging System.

Extraction of total RNA. Exo RNA was isolated using a column-based isolation kit (cat. no. 217184; Qiagen China Co., Ltd.) according to the manufacturer's instructions. Briefly, 1 ml of RNA lysate was added to a 200 μl sample of exosomes, which was subsequently centrifuged at 16,260 x g 4˚C for 90 min, resuspended and precipitated, centrifuged again and then isoacetone and anhydrous ethanol were added in that order. Finally, the RNA was obtained by adding enzyme-free water to resuspend the precipitate. The concentrations were measured using a spectrophotometer(ND-ONE-WA30221; Thermo Fisher Scientific, Inc.) at a wavelength of 260 nm.

Reverse transcription-quantitative (q)PCR. Synthesis of complementary cDNA was performed using an RT kit (cat. no. AG11717; Accurate Biology Inc.;) according to the manufacturer's protocol. The total reaction volume was 20 μl, which included 10 μl 2x miRNA RT Reaction Buffer, 2 μl miRNA RT Enzyme Mix and 8 μl RNA. Thermocycling was performed as follows: 42˚C for 60 min and 95˚C for 3 min. Real-time fluorescent quantitative PCR was performed on a QuanStudio 1 (Thermo Fish Scientific, Inc.) with thermocycling conditions as follows: 95˚C for 30 sec for 1 cycle, and 35 cycles of denaturation at 95˚C for 5 sec, annealing and extension at 60˚C for 30 sec. This process was repeated 3 times for each sample. qPCR was performed using the SYBR Green PCR kit (cat. no. AG11702; Accurate Biology Inc.) according to the manufacturer's protocol. The experiment was performed on a Light Cycle 480 machine (Roche Diagnostics). Each experiment was repeated three times and relative expression levels of miRNA were analyzed using the $2^{-\Delta\Delta Cq}$ method (11). U6 was used for normalization. For RT-qPCR, a tailing method (addition of the poly(A) tail to the 3' end of miRNA by a poly(A) polymerase to increase its length) was used. A specific primer was used upstream and a universal primer was used downstream. All miRNAs were purchased from Tiangen Biotech Co., Ltd. The sequences of the primers used were as follows: has-miR-203 forward (F), 5'-GUGAAA UGUUUAGGACCACUAG-3'; has-miR-4516 F, 5'-GGGAGA AGGGUCGGGGC-3'; and hsa-U6- F, 5'-CTCGCTTCGGCA GCACA-3' and reverse 5'-AACGCTTCACGAATTTGCGT-3'. The miRNA reverse primer was included in the RT-qPCR kit (cat. no. AG11717; Accurate Biology Inc.).

Bioinformatics analysis. Target genes of differentially expressed miRNAs were predicted using TargetScan 8.0 software (https://www.targetscan.org/vert_80/). Kyoto Encyclopedia of Genes and Genomes (https://www.kegg.jp/) enrichment analyses were performed using the David 6.8 online database (https://david.ncifcrf.gov). The ggplot2 package (version 3.3.5) (https://cran.r-project.org/web/packages/ggplot2/) in R (version 4.0.5) (https://www.r-project.org/) was used to plot bar and Venn diagrams for visualization.

Table I. Baseline data of the study participants.

Baseline characteristic	Control, mean ± SD	AMI, mean ± SD	P-value
Age, years	52.81±7.6	62.02±9.46	0.058
HR, beats/min	74.06±11.6	76.76±13.02	0.379
SBP, mmHg	105.03±9.83	125.21±19.58	0.086
DBP, mmHg	79.19±9.77	75.73±14.34	0.277
Cr, μmol/l	75.1±15.73	77.97±15.44	0.289
Glu, mmol/l	5.19±0.74	5.59±1.14	0.054
TG, mmol/l	1.49±0.63	1.49±0.73	0.917
TC, mmol/l	3.96±1.04	4.51±1.03	0.022
LDL, mmol/l	2.69±1.08	2.71±0.81	0.985
HDL, mmol/l	1.21±0.4	1.18±0.47	0.676
Apolipoprotein a, mmol/l	231.83±291.8	330.56±304.14	0.144
Apolipoprotein B, mmol/l	1.01±0.25	1±0.17	0.671
Apolipoprotein E, mmol/l	46.63±12.61	51.59±16.35	0.185

Unpaired Student's t-test was used to assess differences between the AMI and control groups. HR, Heart rate; SBP, Systolic blood pressure; DBP, Diastolic blood pressure; Cr, Creatinine; Glu, Blood glucose; TG, Triglycerides; TC, Total cholesterol; LDL, Low-density lipoprotein; HDL, High-density lipoprotein.

ELISA. Plasma was obtained by centrifuging blood samples at 2,000 x g at 4˚C for 10 min and was then stored at -80˚C. A Human SFRP1 ELISA kit (cat. no. SEF880Hu; Cloud-Clone Corp.) was used to assess the SFRP1 secretion level in each individual, according to the manufacturer's protocols. The signal was measured at 450 nm excitation light using a SpectraMax® i3 multifunctional microplate reader. After the standard curve was established, the plasma expression levels of SFRP1 were calculated based on the absorbance values of each sample.

Statistical analysis. Mean ± standard deviation was used to present relative clinical characteristics. Ordinal variables were compared using one-way ANOVA. The statistical significance of normally distributed data was assessed with the unpaired Student's t-test. Pearson's correlation coefficient was used to validate the relationships between continuous variables. Independent factor risk analysis was performed using logistic regression. All experiments were repeated ≥3 times. All statistical analyses were performed using SPSS software (version 22.0; IBM Corp.) and GraphPad Prism 8.0 (GraphPad Software; Dotmatics). $P<0.05$ was considered to indicate a statistically significant difference.

Table II. Summary of medication use.

Drugs/drug groups (Postoperative)	Control (n=31)	AMI (n=62)
Aspirin, n	12	39
Tegretol, n	NA	NA
Statins, n	4	10
Beta blockers, n	3	22
Proton pump inhibitors, n	NA	20
Isosorbide mononitrate, n	NA	2
ACEI/ARB, n	3	40
Trimetazidine, n	NA	NA
CCB, n	NA	30
Clopidogrel, n	NA	25
Diuretics, n	NA	20
Ivabradine, n	NA	2

ACEI, angiotensin converting enzyme inhibitor; ARB, Angiotensin Receptor Blocker; CCB, calcium Channel Blockers.

Results

Baseline characteristics of the study population. The baseline characteristics of the 31 healthy control individuals and the 62 patients with AMI were summarized (Table I). Unpaired Student's t-test was used to compare the differences between the AMI and control groups. In parallel, drug use data was collected from both groups (Table II). There were no statistically significant differences in these characteristics between the two groups, except for total cholesterol).

Characterization of exos. Previously published reports and the standards of the International Society for Exosome Vesicles indicate that verification of exosomes can be performed using transmission electron microscopy, WB and particle size analysis, simultaneously (34,39). The size and morphology of exosomes can be objectively observed using transmission electron microscopy. Particle size analysis allows the size, diameter and concentration of exosomes to be assessed (40). The typical disc-like structure of exos was observed using TEM, which was a direct observation of plasma exosomes under TEM, whose shape and size met the criteria for exosomes (Fig. 1A). WB allowed verification of specific proteins on the surface of exosomes, such as CD9 and ALIX. Most common cell membranes contain Calnexin proteins; however, exos do

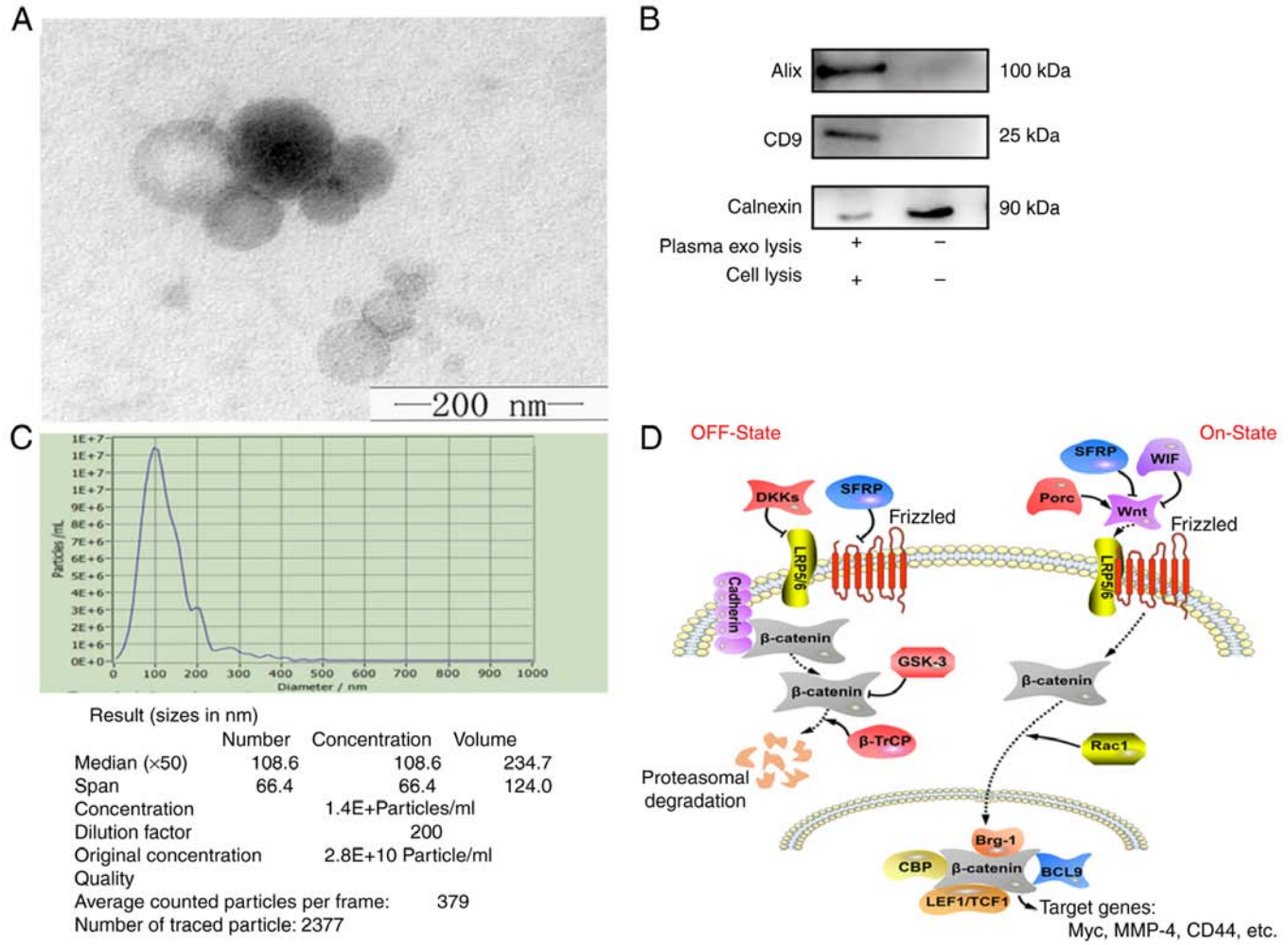

Figure 1. Successful isolation of exos from plasma. (A) Ultrastructure of exos isolated from plasma was examined using transmission electron microscopy. Scale bar=200 nm. (B) The expression of exo markers, Alix and CD9, and the negative marker, calnexin, assessed using western blotting. (C) Size distribution of exos using particle size analysis. (D) SFRP1 serves an inhibitory role in the Wnt/β-Catenin signaling pathway. Exo, exosome; SFRP1, secretory frizzled-related protein 1.

not have Calnexin proteins on their membranes. Therefore, cell lysis was chosen as a control group. The identity of the exos was further confirmed by WB using antibodies against the exo-specific markers, Alix and CD9, and the negative control, calnexin (Fig. 1B). NTA results demonstrated that the average diameter of the isolated granule was 127.5 nm, with a median diameter of 117.7 nm (Fig. 1C), which was in-line with the standard size of exos. These results confirmed that exos were successfully extracted at a high quality and purity. The regulatory relationship between SFRP1 and the Wnt/β-Catenin signaling pathways, which serve a vital role in atherosclerosis or AMI was illustrated (Fig. 1D) (41,42).

Expression levels of exosomal miR-4516, miR-203 and plasma SFRP1 in each study group. Previous sequencing results were analyzed and the top 10 miRNAs with high variance ranking were selected for validation (Fig. 2A) (34). SFRP1 was predicted as the target protein for both miR-4516 and miR-203 using TargetScan software (Fig. 2B). Statistical analysis was performed using an unpaired Student's t-test. The levels of miR-4516 and miR-203 in plasma exos from the AMI group were significantly higher compared with those in the healthy control group. In addition, the SFRP1 protein expression level was significantly increased in the plasma of patients with AMI compared with the control group (Fig. 2C and Tables III-V). These data indicated that exosomal miR-4516, miR-203 and plasma SFRP1 were associated with AMI.

Exosomal miR-4516, miR-203 and plasma SFRP1 levels as diagnostic biomarkers for AMI. The area under the curve (AUC) of exosomal miR-4516 and miR-203 were 0.9809 ($P<0.0001$) and 0.6823 ($P=0.006$), respectively, and the AUC of plasma SFRP1 was 0.9603 ($P<0.0001$) in the AMI group, which indicated that exosomal miR-4516, miR-203 and plasma SFRP1 may be candidate diagnostic biomarkers for AMI (Fig. 2D).

Positive correlation between plasma exosomal miR-4516 and SYNTAX score of patients with AMI. After collecting coronary angiography images from each participant, the images were assessed using the SYNTAX scoring system (Fig. 3A). Plasma exosomal miR-4516 levels were significantly positively correlated with the SYNTAX scores of patients

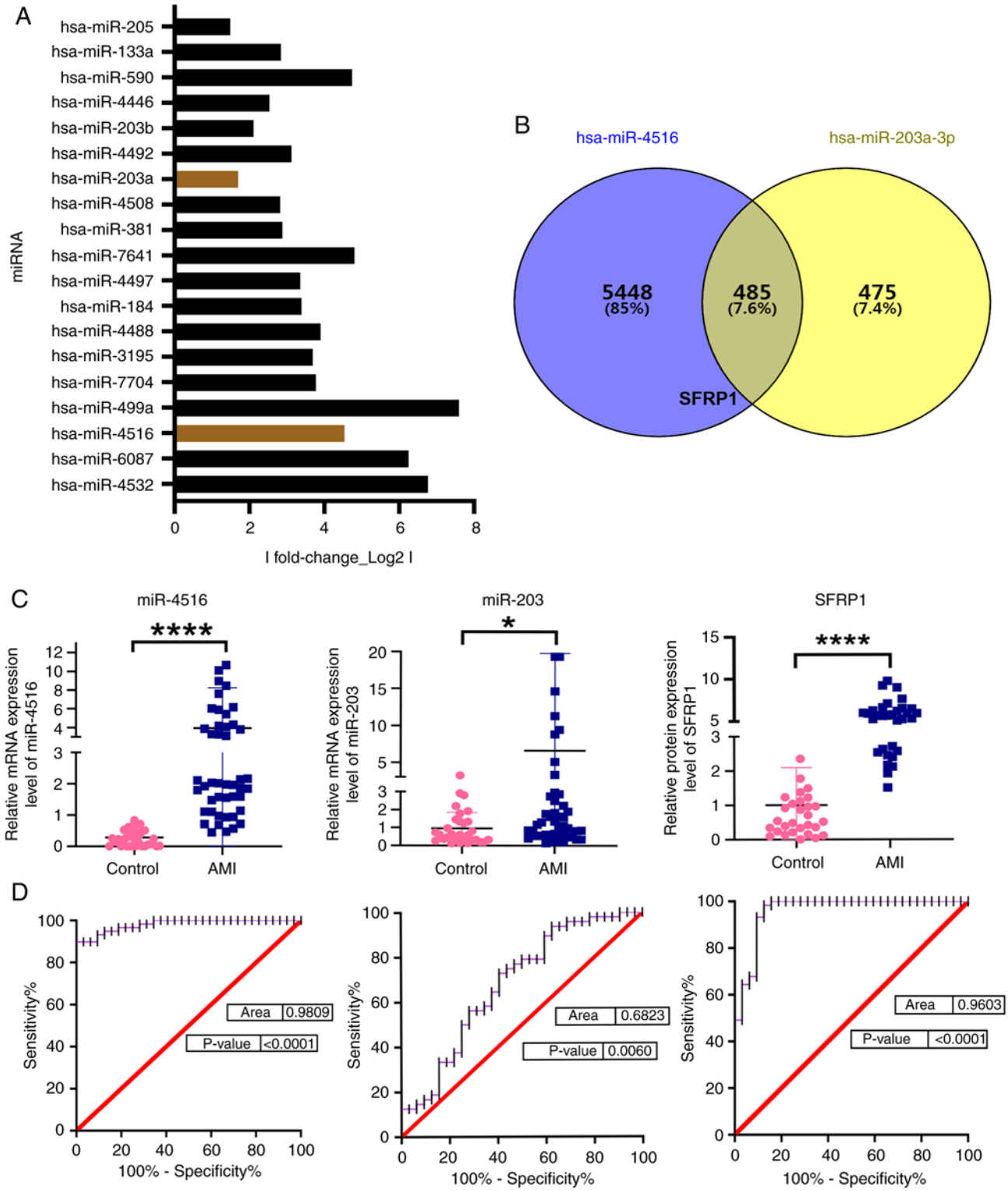

Figure 2. Indicators to diagnose AMI. (A) Previous sequencing results were analyzed and the top 10 miRNAs with high variance rankings were selected for validation. (B) SFRP1 was predicted as a target protein for both miRNAs using TargetScan software. There were 485 predicted downstream target proteins common to mir-4516 and miR-203. (C) Relative expression levels of miR-4516, miR-203 and SFRP1 in different subgroups. Unpaired Student's t-test was used for analysis. (D) Correlation analysis of miR-4516, miR-203 and SFRP1 in diagnosis of AMI. *P<0.05 and ****P<0.001. AMI, acute myocardial infarction; miR, microRNA; miRNA, microRNA; SFRP1, secretory frizzled-related protein 1.

with AMI (r^2=0.7875; P<0.0001) using Pearson's correlation analysis (Fig. 3B). However, there was no significant correlation between either the exosomal miR-203 or plasma SFRP1 levels and the SYNTAX score in the AMI group (r^2=-0.0145, P=0.9461 and r^2=-0.229, P=0.6572, respectively).

Plasma SFRP1 is positively correlated with plasma low-density lipoprotein (LDL) levels in patients with AMI. DBP and LDL of the participants correlated with plasma exosomal miR-4516, miR-203 and SFRP1 levels (Table VI). There was no correlation between the classical marker, cTnI, and plasma exosomal

Table III. SFRP1 expression levels in AMI and control groups.

Group	Standard error	Mean deviation	P-value	95% Confidence interval	
				Lower	Upper
Control (miR-4516)	4.284	0.272	0.001	0.176	0.368
AMI (miR-4516)	0.270	3.871	0.001	2.640	5.102
Control (miR-203)	3.578	2.387	0.001	1.359	3.415
AMI (miR-203)	1.171	1.050	0.001	0.659	1.440
Control (SFRP1)	1.802	4.657	0.001	4.196	5.119
AMI (SFRP1)	1.111	1.017	0.001	0.610	1.425

AMI, acute myocardial infarction; miR, microRNA; SFRP1, secretory frizzled-related protein 1.

Table IV. MiR-203 expression levels in AMI and control groups.

Group	Standard error	Mean deviation	P-value	95% Confidence interval	
				Lower	Upper
Control	3.578	2.387	0.001	1.359	3.415
AMI	1.171	1.050	0.001	0.659	1.440

AMI, acute myocardial infarction.

Table V. Secretory frizzled-related protein 1expression levels in AMI and control groups.

Group	Standard error	Mean deviation	P-value	95% Confidence interval	
				Lower	Upper
Control	1.802	4.657	0.001	4.196	5.119
AMI	1.110	1.017	0.001	0.610	1.425

AMI, acute myocardial infarction.

miR-4516, miR-203 and SFRP1 levels (Fig. 3C). Plasma SFRP1 was positively correlated with serum LDL levels (r^2=0.667; P=0.0415); however, there was no correlation between plasma exosomal miR-4516 or miR-203 and serum LDL levels (Fig. 3D). A logistic regression analysis of common risk factors for coronary artery disease was performed.

miR-4516 and miR-203 are associated with adhesion. The KEGG enrichment analysis demonstrated that miR-4516 and miR-203 shared 748 enrichment pathways, and that miR-4516 and miR-203 were associated with adhesion function in the enriched pathways (Fig. 4A and B).

Discussion

CVD remains one of the leading causes of death worldwide, and AMI is the most aggressive and problematic type of CVD (1). With health education and the continuous innovation of testing equipment, there is an increased awareness of early diagnosis and early treatment of AMI (43). Survival rates for AMI are gradually improving in developed cities, However, the relative lack of diagnostic capacity for AMI in less developed regions and the poor access to treatment increase the mortality rate of patients with AMI. Classical plasma markers of AMI, such as cTnI and CK-MB, are becoming less specific and have certain drawbacks in clinical diagnosis. This is due to multiple co-morbidities, such as myocarditis, heart failure and pulmonary heart disease, which also cause elevations in these markers (44). Exos are the products of cellular secretion and are found in large numbers in various bodily fluids and reflect intracellular status in real time. Previous studies have reported that the miRNAs transported in exos are of significant value in various CVDs. For example, miR-133, miR-146, miR-499 and miR-26a in plasma can be used as potential diagnostic markers for AMI (45).

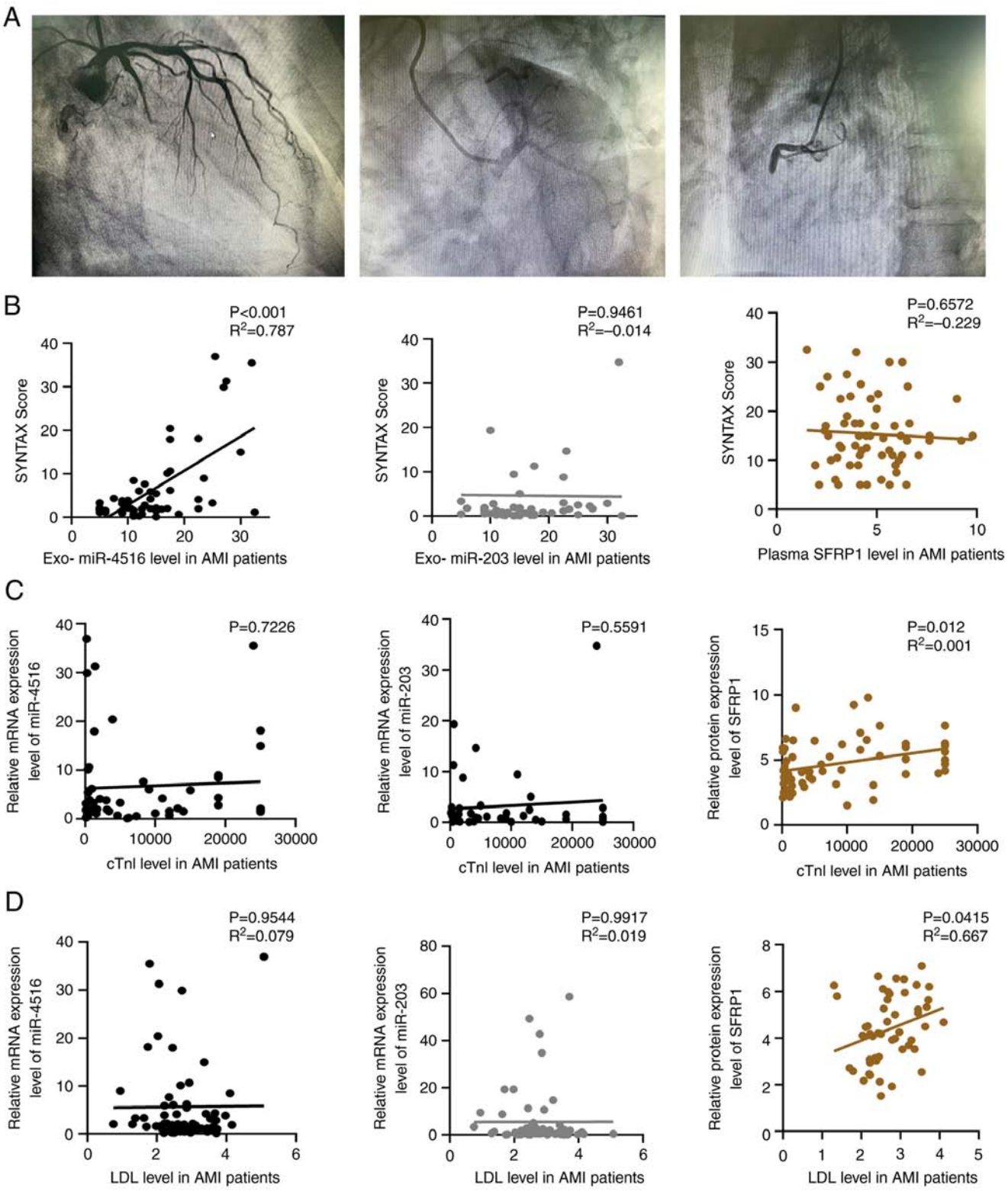

Figure 3. Correlation of plasma exosomal miR-4516, miR-203 and SFRP1 levels with SYNATX scores. (A) Representative images from a coronary angiography procedure. The three images show (left to right) occlusion of the gyral, anterior descending and right coronary branches of the left coronary artery, respectively. The degree of damage to the vessel was predicted based on the blockage and was assessed using the SYNATX score. (B) Correlation analysis of plasma exosomal miR-4516, miR-203 and SFRP1 levels with the SYNATX score of patients with AMI. Correlation of plasma exosomal miR-4516, miR-203 and SFRP1 levels with (C) cTnI and (D) LDL in patients with AMI. AMI, acute myocardial infarction; cTnI, cardiac troponin I; exo, exosome; LDL, low-density lipoprotein; miR, microRNA; SFRP1, secretory frizzled-related protein 1.

In the present study, TargetScan predicted that SFRP1 may be a target protein for miR-4516 and miR-203. The results of the present study demonstrated that the expression levels of the three indicators were significantly elevated in the AMI group compared with the control, which prompted the hypothesis of a relationship between the three indicators and AMI. Pearson's

Table VI. Correlations between serum exosomal miR-4516, miR-203 and SRFP1 levels and traditional risk factors of cardiovascular diseases in AMI patients.

		Exosomal miR-4516		Exosomal miR-203		SRFP1	
Characteristics	Value	Control	AMI	Control	AMI	Control	AMI
Age, years	P	0.802	0.918	0.746	0.994	0.691	0.175
	R^2	-0.051	-0.015	0.160	0.007	0.573	-0.025
HR, beats/min	P	0.492	0.572	0.374	0.434	0.361	0.775
	R^2	-0.189	-0.109	0.5876	-0.103	0.175	0.005
SBP, mmHg	P	0.590	0.222	0.081	0.076	0.003	0.984
	R^2	0.206	0.342	-1.567	0.359	0.737	0.001
DBP, mmHg	P	0.420	0.842	0.842	0.014	0.616	0.804
	R^2	0.193	0.042	0.115	0.376	-0.843	0.003
Cr, μmol/l	P	0.051	0.172	0.871	0.694	0.213	0.732
	R^2	-0.706	0.313	-0.145	0.066	0.321	-0.004
Glu, mmol/l	P	0.223	0.051	0.365	0.128	0.986	0.663
	R^2	0.021	-0.032	0.037	0.018	-0.002	0.091
TG, mmol/l	P	0.867	0.085	0.835	0.933	0.374	0.731
	R^2	0.002	0.018	0.007	0.001	-0.091	0.118
TC, mmol/l	P	0.378	0.980	0.609	0.940	0.075	0.180
	R^2	0.021	0.001	-0.029	0.001	0.296	0.319
LDL, mmol/l	P	0.939	0.954	0.446	0.991	0.934	0.041
	R^2	-0.001	0.001	-0.046	0.091	-0.014	0.677
HDL, mmol/l	P	0.847	0.306	0.212	0.590	0.761	0.977
	R^2	-0.001	-0.007	-0.028	0.003	-0.02	0.012
Apolipoprotein a	P	0.592	0.223	0.476	0.193	0.554	0.092
	R^2	-3.757	0.005	0.119	-0.042	-0.29	0.001
Apolipoprotein B	P	0.817	0.855	0.533	0.902	0.747	0.111
	R^2	0.001	-0.004	-0.008	0.002	-0.013	0.028
Apolipoprotein E	P	0.259	0.489	0.828	0.994	0.311	0.952
	R^2	0.336	0.17	0.156	0.001	-0.211	0.001

AMI, acute myocardial infarction; miR, microRNA; SFRP1, secretory frizzled-related protein; SBP, Systolic blood pressure; DBP, Diastolic blood pressure; Cr, Creatinine; Glu, Blood glucose; TG, Triglycerides; TC, Total cholesterol; LDL, Low-density lipoprotein; HDL, High-density lipoprotein.

correlation analysis further demonstrated that exosomal levels of miR-4516 and miR-203 and plasma SFRP1 levels were significantly correlated with AMI.

Coronary angiography can not only determine whether a coronary artery is blocked and the extent of obstruction, but also support the selection of a protocol for the next step of treatment. SYNTAX scores can be used to quantitatively evaluate the complexity of coronary lesions and provide a preliminary judgment, which can inform the choice of the surgical procedure according to a specific scoring system based on anatomical characteristics, such as coronary lesion location, severity, bifurcation and calcification. In addition, patients with MI often have multiple co-morbidities, such as heart failure, anemia or even uremia at an advanced age. Both ST-segment elevation myocardial infarction and non-ST-segment elevation myocardial infarction have corresponding blocked blood vessels, which can be identified on late coronary angiography. Where this occurs, it would be advantageous if the severity of the lesioned vessel could be determined as early as possible in conjunction with the SYNTAX score. Early assessment of the severity of the blockage in the vessel can predict the severity of damage to the heart muscle. For example, if the blockage is small, thrombolytic therapy may be an immediate option. However, if the blockage is severe and combined with chronic occlusion of multiple vessels, cardiac bypass surgery may be the immediate treatment of choice (46,47). In the present study, the relationship between the expression levels of exosomal miR-4516, miR-203 and SFRP1 in the AMI group with their SYNTAX scores were analyzed. Correlation analysis demonstrated that only miR-4516 was significantly positively correlated with the SYNTAX score of patients with AMI, and that neither miR-203 nor SFRP1 were correlated with SYNTAX score (48,49). These data indicated that exosomal miR-4516 may be used as a non-invasive means of predicting the lesion complexity of coronary vessels in patients with AMI, providing an initial basis for the next treatment step (PCI or coronary artery bypass

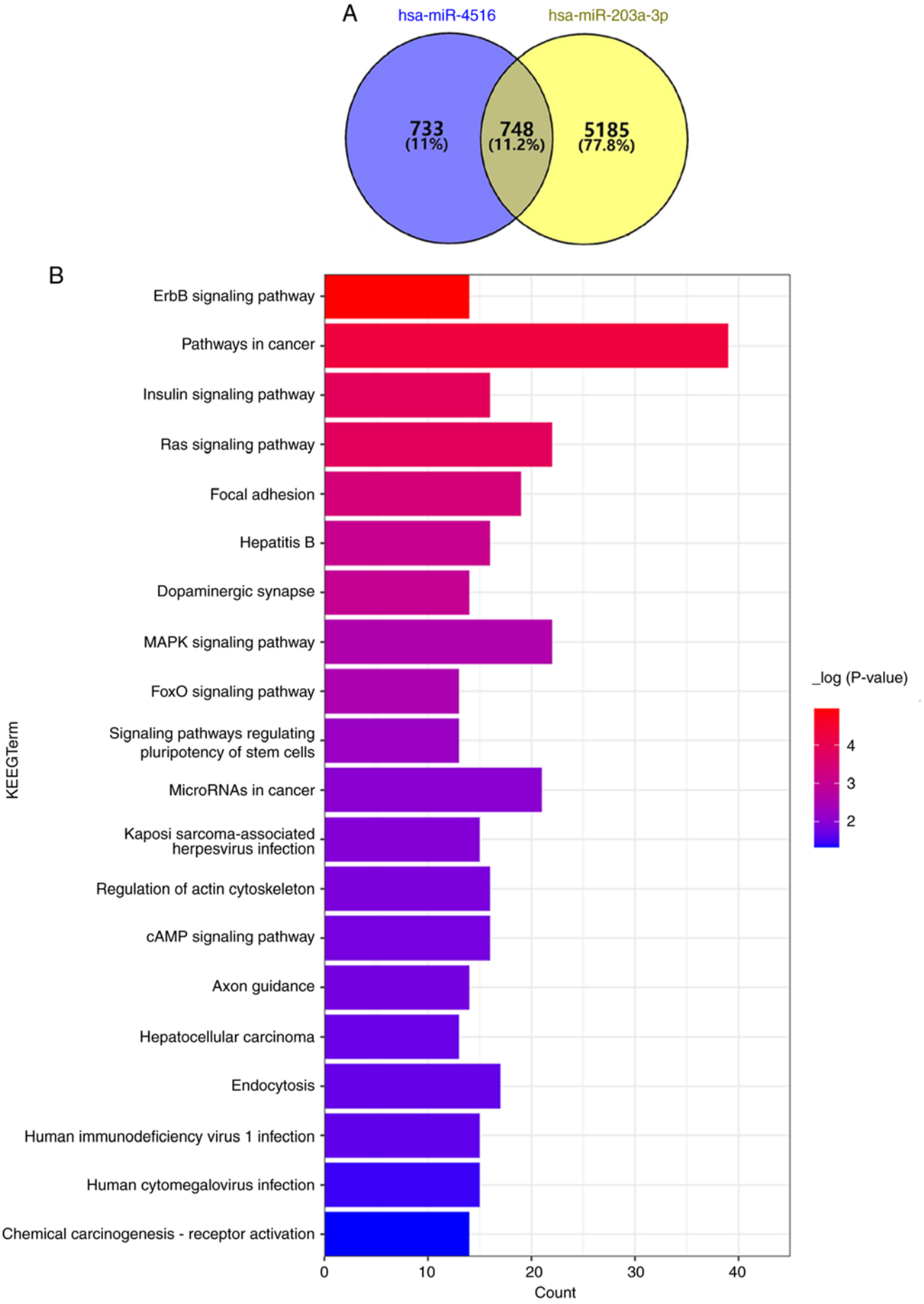

Figure 4. Bioinformatic analysis. (A) MiR-4516 and miR-203 shared 748 identical enrichment pathways. (B) Among the first 20 enrichment pathways, there was an association of miR-4516 and miR-203 with adhesion. KEGG, Kyoto Encyclopedia of Genes and Genomes; miR, microRNA.

grafting). The elevation of LDL in plasma is considered to be a major risk factor for atherosclerosis, and the most direct cause of AMI is the rupture of the atherosclerotic plate. Notably, in the present study, Pearson's correlation analysis demonstrated that SFRP1 protein expression levels were significantly correlated with LDL. After statistical analysis, no correlation was demonstrated between SFRP1 mRNA expression levels and SYNTAX scores, but the AMI group had significantly higher SFRP1 protein expression levels compared with the control group. Statistical analysis demonstrated that SFRP1 protein expression levels were significantly correlated with cTNl. As SFRP1 is a key protein in the WNT signaling pathway, it was hypothesized that SFRP1 may be positively correlated with the severity of cardiomyocyte injury and angiogenesis (42). In addition to this, based on the results of the present study, it was hypothesized that SFRP1 may be involved in lipid metabolism. However, for reasons of time, further validation was not performed.

Both miRNAs, miR-4516 and miR-203, were predicted by bioinformatic analysis to be closely associated with adhesion and endocytosis. The present study could not distinguish between STEMI and non-STEMI as the subsequent treatment regimens for these two types of AMI are different. Moreover, the detection of miRNA in plasma exos was quite time-consuming. The time must be decreased to facilitate use in a clinical setting. The main reason for this is that the process of exo extraction takes about one hour. SYNTAX 2 scores combine the clinical variables of the patient, such as sex, age, left ventricular ejection fraction, creatinine clearance and other information, which allow accurate evaluation of the condition of the patient (38). Therefore, combination of the difference in exosomal miRNA and SYNTAX 2 scores facilitates a more personalized treatment plan for patients.

The present study had limitations including that at the time of diagnosis of AMI, all patients had the necessary tests for cTnl and ECG. Obtaining the results of tests such as CK-MB and BNP was slow compared with cTnl, and we did not consider these as a necessary test considering that it would delay the patient's treatment; therefore, the data for these two indicators are relatively incomplete. The plasma samples collected were of human origin and as such the composition of the plasma was complex and, even if some of the more biased samples are excluded, the dispersion of some of the samples was still large, this was also a limitation of the present study. In addition to this, another limitation of the present study was the lack of data and survival information related to the later stages of recovery from myocardial infarction in patients. Therefore, no relevant prognostic and survival analysis were performed for this.

In conclusion, a combination of miR-4516, miR-203 and SFRP1 may help in the diagnosis of AMI and in the evaluation of the degree of coronary stenosis. Furthermore, the present study demonstrated a significant correlation between plasma SFRP1 protein expression levels and LDL levels. These results may provide novel diagnostic markers for AMI, which may contribute to the timely diagnosis and treatment of AMI.

Acknowledgements

The authors would like to thank Dr Yan Zheng (Research Center of Translational Medicine, Central Hospital Affiliated to Shandong First Medical University, Jinan, Shandong, China) for their technical assistance.

Funding

This work was supported by the Natural Science Foundation of Shandong Province (grant no. ZR202103050087).

Availability of data and materials

The datasets used and/or analyzed during the present study are available from the corresponding author on reasonable request.

Authors' contributions

PL, KL and SW designed the present study, searched databases, extracted and assessed the literature and drafted the manuscript. PL, JT, YY, LW and YM statistically analyzed the data. YY and LW confirm the authenticity of all the raw data. PL, FD and GS conceived and designed the present study, provided general supervision and finalized the manuscript. All authors read and approved the final manuscript.

Ethics approval and consent to participate

The present study was approved by the ethics committee of Jinan Central Hospital (approval no. 2018-039-01).

Patient consent for publication

Not applicable.

Competing interests

The authors declare that they have no competing interests.

References

1. Zhao D, Liu J, Wang M, Zhang X and Zhou M: Epidemiology of cardiovascular disease in China: Current features and implications. Nat Rev Cardiol 16: 203-212, 2019.
2. Ma LY, Chen WW, Gao RL, Liu LS, Zhu ML, Wang YJ, Wu ZS, Li HJ, Gu DF, Yang YJ, *et al*: China cardiovascular diseases report 2018: An updated summary. J Geriatr Cardiol 17: 1-8, 2020.
3. Bhatnagar P, Wickramasinghe K, Wilkins E and Townsend N: Trends in the epidemiology of cardiovascular disease in the UK. Heart 102: 1945-1952, 2016.
4. Rozenman Y and Gotsman MS: The earliest diagnosis of acute myocardial infarction. Annu Rev Med 45: 31-44, 1994.
5. Menown IB, Allen J, Anderson JM and Adgey AA: ST depression only on the initial 12-lead ECG: Early diagnosis of acute myocardial infarction. Eur Heart J 22: 218-227, 2001.
6. Kim SJ, Kim MH, Lee KM, Kim TH, Choi SY, Son MK, Park JW and Serebruany VL: Troponin I and D-dimer for discriminating acute pulmonary thromboembolism from myocardial infarction. Cardiology 136: 222-227, 2017.
7. Roongsritong C, Warraich I and Bradley C: Common causes of troponin elevations in the absence of acute myocardial infarction: Incidence and clinical significance. Chest 125: 1877-1884, 2004.
8. Waters RE II, Singh KP, Roe MT, Lotfi M, Sketch MH Jr, Mahaffey KW, Newby LK, Alexander JH, Harrington RA, Califf RM and Granger CB: Rationale and strategies for implementing community-based transfer protocols for primary percutaneous coronary intervention for acute ST-segment elevation myocardial infarction. J Am Coll Cardiol 43: 2153-2159, 2004.
9. Pegtel DM and Gould SJ: Exosomes. Annu Rev Biochem 88: 487-514, 2019.

10. Tang YT, Huang YY, Zheng L, Qin SH, Xu XP, An TX, Xu Y, Wu YS, Hu XM, Ping BH and Wang Q: Comparison of isolation methods of exosomes and exosomal RNA from cell culture medium and serum. Int J Mol Med 40: 834-844, 2017.
11. Liu Y, Sun Y, Lin X, Zhang D, Hu C, Liu J, Zhu Y, Gao A, Han H, Chai M, *et al*: Perivascular adipose-derived exosomes reduce macrophage foam cell formation through miR-382-5p and the BMP4-PPARγ-ABCA1/ABCG1 pathways. Vascul Pharmacol 143: 106968, 2022.
12. Zhu J, Liu B, Wang Z, Wang D, Ni H, Zhang L and Wang Y: Exosomes from nicotine-stimulated macrophages accelerate atherosclerosis through miR-21-3p/PTEN-mediated VSMC migration and proliferation. Theranostics 9: 6901-6919, 2019.
13. Zhang J, Li S, Li L, Li M, Guo C, Yao J and Mi S: Exosome and exosomal microRNA: Trafficking, sorting, and function. Genomics Proteomics Bioinformatics 13: 17-24, 2015.
14. Ambros V: The functions of animal microRNAs. Nature 431: 350-355, 2004.
15. Mishra S, Yadav T and Rani V: Exploring miRNA based approaches in cancer diagnostics and therapeutics. Crit Rev Oncol Hematol 98: 12-23, 2016.
16. Turchinovich A, Weiz L, Langheinz A and Burwinkel B: Characterization of extracellular circulating microRNA. Nucleic Acids Res 39: 7223-7233, 2011.
17. Lu TX and Rothenberg ME: MicroRNA. J Allergy Clin Immunol 141: 1202-1207, 2018.
18. Li Y, Ren S, Xia J, Wei Y and Xi Y: EIF4A3-Induced circ-BNIP3 aggravated hypoxia-induced injury of H9c2 cells by targeting miR-27a-3p/BNIP3. Mol Ther Nucleic Acids 19: 533-545, 2020.
19. Al-Muhtaresh HA, Salem AH and Al-Kafaji G: Upregulation of circulating cardiomyocyte-enriched miR-1 and miR-133 associate with the risk of coronary artery disease in type 2 diabetes patients and serve as potential biomarkers. J Cardiovasc Transl Res 12: 347-357, 2019.
20. Ren J, Zhang J, Xu N, Han G, Geng Q, Song J, Li S, Zhao J and Chen H: Signature of circulating microRNAs as potential biomarkers in vulnerable coronary artery disease. PLoS One 8: e80738, 2013.
21. Wiese CB, Zhong J, Xu ZQ, Zhang Y, Ramirez Solano MA, Zhu W, Linton MF, Sheng Q, Kon V and Vickers KC: Dual inhibition of endothelial miR-92a-3p and miR-489-3p reduces renal injury-associated atherosclerosis. Atherosclerosis 282: 121-131, 2019.
22. Stone GW, Sabik JF, Serruys PW, Simonton CA, Généreux P, Puskas J, Kandzari DE, Morice MC, Lembo N, Brown WM III, *et al*: Everolimus-eluting stents or bypass surgery for left main coronary artery disease. N Engl J Med 375: 2223-2235, 2016.
23. Suh YJ, Hong YJ, Lee HJ, Hur J, Kim YJ, Lee HS, Hong SR, Im DJ, Kim YJ, Park CH, *et al*: Prognostic value of SYNTAX score based on coronary computed tomography angiography. Int J Cardiol 199: 460-466, 2015.
24. Clevers H and Nusse R: Wnt/β-catenin signaling and disease. Cell 149: 1192-1205, 2012.
25. Liu Y, Almeida M, Weinstein RS, O'Brien CA, Manolagas SC and Jilka RL: Skeletal inflammation and attenuation of Wnt signaling, Wnt ligand expression, and bone formation in atherosclerotic ApoE-null mice. Am J Physiol Endocrinol Metab 310: E762-E773, 2016.
26. Torres VI, Godoy JA and Inestrosa NC: Modulating Wnt signaling at the root: Porcupine and Wnt acylation. Pharmacol Ther 198: 34-45, 2019.
27. Zhang L and Wrana JL: The emerging role of exosomes in Wnt secretion and transport. Curr Opin Genet Dev 27: 14-19, 2014.
28. Yang Y and Mlodzik M: Wnt-Frizzled/planar cell polarity signaling: Cellular orientation by facing the wind (Wnt). Annu Rev Cell Dev Biol 31: 623-646, 2015.
29. Tsutsumi N, Mukherjee S, Waghray D, Janda CY, Jude KM, Miao Y, Burg JS, Aduri NG, Kossiakoff AA, Gati C and Garcia KC: Structure of human Frizzled5 by fiducial-assisted cryo-EM supports a heterodimeric mechanism of canonical Wnt signaling. Elife 9: e58464, 2020.
30. Kobayashi K, Luo M, Zhang Y, Wilkes DC, Ge G, Grieskamp T, Yamada C, Liu TC, Huang G, Basson CT, *et al*: Secreted Frizzled-related protein 2 is a procollagen C proteinase enhancer with a role in fibrosis associated with myocardial infarction. Nat Cell Biol 11: 46-55, 2009.
31. Barandon L, Casassus F, Leroux L, Moreau C, Allières C, Lamazière JM, Dufourcq P, Couffinhal T and Duplàa C: Secreted frizzled-related protein-1 improves postinfarction scar formation through a modulation of inflammatory response. Arterioscler Thromb Vasc Biol 31: e80-e87, 2011.
32. Sassi Y, Avramopoulos P, Ramanujam D, Grüter L, Werfel S, Giosele S, Brunner AD, Esfandyari D, Papadopoulou AS, De Strooper B, *et al*: Cardiac myocyte miR-29 promotes pathological remodeling of the heart by activating Wnt signaling. Nat Commun 8: 1614, 2017.
33. Liu J, Zheng X, Zhang C, Zhang C and Bu P: Lcz696 alleviates myocardial fibrosis after myocardial infarction through the sFRP-1/Wnt/β-catenin signaling pathway. Front Pharmacol 12: 724147, 2021.
34. Liu P, Wang S, Wang G, Zhao M, Du F, Li K, Wang L, Wu H, Chen J, Yang Y and Su G: Macrophage-derived exosomal miR-4532 promotes endothelial cells injury by targeting SP1 and NF-κB P65 signalling activation. J Cell Mol Med 26: 5165-5180, 2022.
35. Alpert JS, Thygesen K, Antman E and Bassand JP: Myocardial infarction redefined-a consensus document of the joint european society of cardiology/American college of cardiology committee for the redefinition of myocardial infarction. J Am Coll Cardiol 36: 959-969, 2000.
36. Saraiva JFK and Franco D: Oral GLP-1 analogue: Perspectives and impact on atherosclerosis in type 2 diabetic patients. Cardiovasc Diabetol 20: 235, 2021.
37. Biagini A, Testa R, Carpeggiani C, Andreotti F, Mazzei MG, Emdin M and L'Abbate A: Detection of spontaneous episodes in post-infarction angina. Comparison between CCU and Holter monitoring. Eur Heart J 7 (Suppl 3): S43-S46, 1986.
38. Kundu A, Sardar P, O'Day K, Chatterjee S, Owan T and Dawn Abbott J: SYNTAX score and outcomes of coronary revascularization in diabetic patients. Curr Cardiol Rep 20: 28, 2018.
39. Théry C, Witwer KW, Aikawa E, Alcaraz MJ, Anderson JD, Andriantsitohaina R, Antoniou A, Arab T, Archer F, Atkin-Smith GK, *et al*: Minimal information for studies of extracellular vesicles 2018 (MISEV2018): A position statement of the international society for extracellular vesicles and update of the MISEV2014 guidelines. J Extracell Vesicles 7: 1535750, 2018.
40. Kalluri R and LeBleu VS: The biology, function, and biomedical applications of exosomes. Science 367: eaau6977, 2020.
41. Yu X, Rong PZ, Song MS, Shi ZW, Feng G, Chen XJ, Shi L, Wang CH and Pang QJ: lncRNA SNHG1 induced by SP1 regulates bone remodeling and angiogenesis via sponging miR-181c-5p and modulating SFRP1/Wnt signaling pathway. Mol Med 27: 141, 2021.
42. Mafakher L, Rismani E, Rahimi H, Enayatkhani M, Azadmanesh K and Teimoori-Toolabi L: Computational design of antagonist peptides based on the structure of secreted frizzled-related protein-1 (SFRP1) aiming to inhibit Wnt signaling pathway. J Biomol Struct Dyn 40: 2169-2188, 2022.
43. Zhu L, Liu F, Xie H and Feng J: Diagnostic performance of microRNA-133a in acute myocardial infarction: A meta-analysis. Cardiol J 25: 260-267, 2018.
44. Xing X, Guo S, Zhang G, Liu Y, Bi S, Wang X and Lu Q: miR-26a-5p protects against myocardial ischemia/reperfusion injury by regulating the PTEN/PI3K/AKT signaling pathway. Braz J Med Biol Res 53: e9106, 2020.
45. Xin Y, Yang C and Han Z: Circulating miR-499 as a potential biomarker for acute myocardial infarction. Ann Transl Med 4: 135, 2016.
46. Duijvesz D, Luider T, Bangma CH and Jenster G: Exosomes as biomarker treasure chests for prostate cancer. Eur Urol 59: 823-831, 2011.
47. Lin B, Tian T, Lu Y, Liu D, Huang M, Zhu L, Zhu Z, Song Y and Yang C: Tracing tumor-derived exosomal PD-L1 by dual-aptamer activated proximity-induced droplet digital PCR. Angew Chem Int Ed Engl 60: 7582-7586, 2021.
48. Thuijs DJFM, Kappetein AP, Serruys PW, Mohr FW, Morice MC, Mack MJ, Holmes DR Jr, Curzen N, Davierwala P, Noack T, *et al*: Percutaneous coronary intervention versus coronary artery bypass grafting in patients with three-vessel or left main coronary artery disease: 10-Year follow-up of the multicentre randomised controlled SYNTAX trial. Lancet 394: 1325-1334, 2019.
49. Duttagupta S, Thachathodiyl R, Rameshan A, Venkatachalam A, Georgy S, Ts D and Menon J: Effectiveness of Framingham and ASCVD risk scores in predicting coronary artery disease-a comparative study with syntax score. J Assoc Physicians India 69: 11-12, 2022.